Audio Engineering Society

Convention Express Paper 201

Presented at the 156th Convention

2024 June 15-17, Madrid, Spain

A NEW METRIC FOR LOUDSPEAKER FORCE FACTOR SYMMETRY ANALYSIS

Dario Cinanni

Correspondence should be addressed to Author (Cinanni.AES156@gmail.com)

ABSTRACT

Excluding problems linked to geometries and materials, loudspeakers distortion produced at high signal amplitudes is mainly due to motor and suspensions system asymmetries. A novel metric is introduced to examine loudspeaker *BL* asymmetries that generate 2nd-order Inter Modulation Distortion and Harmonic Distortion. With the new metric is possible to recognize new type of asymmetries and their small differences, offering a measure of them, point-by-point or integrated in a specific region. Moreover, the used scale is an absolute quantity, making it valuable for comparing loudspeakers performances referred to general asymmetries, optimizing or selecting among various designs of the same loudspeaker. The practical application of this method is demonstrated examining a loudspeaker motor force factor *BL(x)*, plotting and discussing asymmetries for different voice coil rest positions and *XBL* displacement.

1 Background

As we know from IEC EN 62458 Standard [1], W. Klippel papers [2], [3], [4] and application note [5] the loudspeaker optimal voice coil rest position can be found by investigating the force factor (*BL*) asymmetry and symmetry region. Then a particular importance is given to the symmetry point, called x_{sym}, of the *BL(x)* curve. In the aforementioned references the *BL asymmetry* (A_{BL}) is defined as:

$$A_{BL}(x_{ac}, x_{off}) = \frac{BL(x_{off}+x_{ac})-BL(x_{off}-x_{ac})}{BL(x_{off}+x_{ac})+BL(x_{off}-x_{ac})} 100\ \% \qquad (1)$$

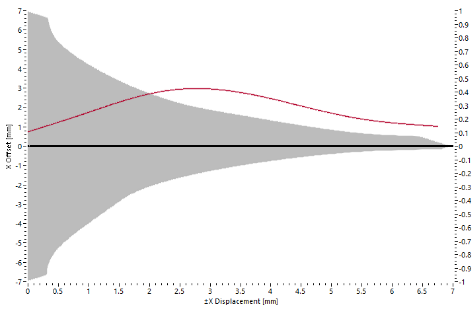

Figure 1. *BL asymmetry* graph. The scale of the axis of ordinates is magnified on the right side and it relates to x_{sym} (red line).

Where x_{ac} and x_{off} are respectively the amplitude displacement and the virtual offset, both related to the voice coil rest position. The recommendation for the rest position is to preserve the absolute value of *BL asymmetry* (A_{BL}) below 5 %, as reported in the grey region of the Fig. 1.

2 Current Metric

Inside these limits we want to investigate in deep what is the difference in changing voice coil offset and its symmetry point, creating a new tool for comparing offset asymmetries.

After the analysis of different metrics for error evaluation, the Symmetric Mean Absolute Percentage Error (*SMAPE*) formula is selected, it permits to obtain also a unique number for asymmetries classification.

$$SMAPE = n^{-1} \sum_{t=1}^{n} \frac{|A_t - F_t|}{|A_t| + |F_t|} 100\ \% \qquad (2)$$

Where A_t is the actual value and F_t is the forecast value. This is the widely used *SMAPE 100 %* expression. It is applied usually for time series in

forecast, machine learning or neural networks accuracy measures. The *SAPE* denominator is not divided by half the sum of actual and forecast values bringing to the *200 %* expression of *SMAPE*, likewise it is not the original "adjusted *MAPE*" proposed by Armstrong [6] in 1985 without the absolute values in denominator, bringing to negative error values giving it an ambiguous interpretation.
SMAPE advantages are the scale-independency and interpretability and its formulation permits to obtain a direct link to the loudspeaker *BL* modulation distortion, according to Clause 24 of IEC 60268-5 [7] for a two-tone signal comprising a tone at resonance frequency *f1= fs* and a second tone at *f2=* 8,5 *fs*. Consequently, it is possible to use *SMAPE* to estimate loudspeaker non-linearities due to *BL(x)* asymmetries in addition the scale-independency permits to compare results among loudspeakers optimizing loudspeaker design.
It is not a coincidence that the right side of (1) is similar to the *SAPE* term of (2), but like the *APE* formula outliers, the two well-known disadvantages [8] of the *SMAPE* formula are that it produces unstable results for extremely small input values, moreover when both inputs are zero the output is undefined, due to the zeroes ratio.
Particularly, the last disadvantage is a great limit in case of intermittent data series in forecast predictions. If a time data or in general a series of data has zero or close to zero values, the analysis using *SMAPE* presents undefined values or high peaks on these points, giving a wrong bias result.
In loudspeaker field, outside the voice coil rest position a *BL(x)* profile could have values close to zero i. e. towards its extreme bounds when voice coil wire is small, or else a zero crossing in case of required or undesired magnetic breaks.
On these points the asymmetry evaluation using (2) brings to a kind of graph showed in Fig. 2.

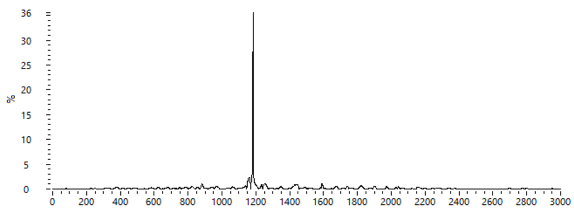

Figure 2. Error measure using *SMAPE* function between two series (3000 points) with similar data, approximately symmetrical, having close to zero input values near to point 1200

3 New Metric

Introducing a new metric:

$$wSMAPE = n^{-1} \sum_{t=1}^{n} wSAPE \;\; 100\,\% \qquad (3)$$

$$wSAPE = \frac{|x-y|}{\varepsilon + |x| + |y|} \qquad (4)$$

Where x and y of (3) are respectively A_t and F_t terms of the *SMAPE* (2) function. The *wSAPE* range is (0,1) and the new term ε in (4) represents the weighting filter of the *SMAPE* (2) function:

$$\varepsilon = \left(\frac{1}{1+|x|+|y|+||x|-|y||}\right)^{\delta} \qquad (5)$$

The benefit of this filter (5) is that it acts on *SMAPE* only for zero and close to zero values, leaving unchanged all other values. δ is the *Quality Factor* of the filter. We can fix the value of $\delta = 21$ obtaining a first function we can call *fixed-weight filter SMAPE* (***FWSMAPE*** or ***fwSMAPE***), using it as a general function for the widely held data series, Fig. 3.

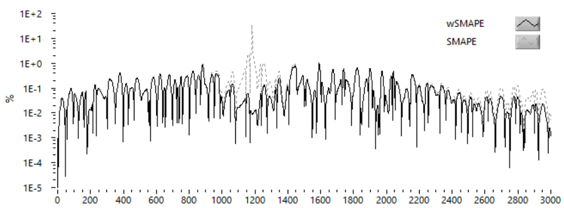

Figure 3. *SMAPE* of Fig. 2 (dashed grey line), compared to new *wSMAPE*, fixed-weight $\delta = 21$ filter (black line). Here % is mapped in logarithmic scale for a better visualization.

In general, the lower the value for Symmetric Mean Absolute Percentage Error the better is the accuracy of the model, but there is not a common value for all applications, the right value depends on the type of industry and in some cases from the company type. Moreover, the nature of input data, their units and the lower extension vary, for this reason it is necessary to increase or reduce the filter bandwidth, to adapt filter to data. Indeed, as showed in Fig. 3 using the *fwSMAPE* it attenuates error for close-to-zero input values nearby point 1200, moreover it applies an underestimation error bias starting also from point 2200 up, in which different amplitudes of close-to-zero inputs are present.
For a better calibration a new function is given, we can call it variable-weight filter *SMAPE* (***VWSMAPE*** or ***vwSMAPE***) using a variable δ

$$\delta = \frac{1100-k}{k} \quad (6)$$

$selecting\ k\ in\ so\ as\ \forall k \in \mathbb{R}:\ 0 < k \leq 100$
where:

$$\lim_{k \to 0} \delta = +\infty \xrightarrow{yields} vwSMAPE \equiv SMAPE$$

$$\lim_{k \to 100} \delta = 10 \xrightarrow{yields} vwSMAPE\ max\ filter\ weight$$

A lower value of the *Quality Factor* δ corresponds to a wider bandwidth and when $k = 100$ it has the maximum impact on the *vwSMAPE* function.
In equivalent manner a higher value of the *Quality Factor* δ corresponds to a narrower bandwidth. For $k = 0$ the *vwSMAPE* filter is switched off because the term ε in the *vwSMAPE* function disappears leaving *vwSMAPE* like the well-known *SMAPE* expression, paying attention to the division by 0 in (6), and that all benefits of the *vwSMAPE* disappear too.

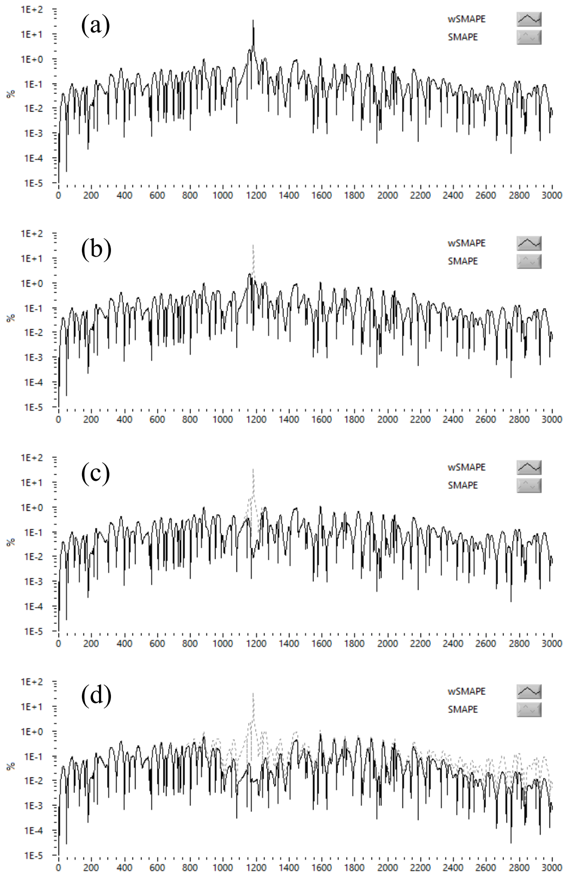

Figure 4. $k = 0$, filter switched off (a). $k = 1$ (b). $k = 10$ (c). $k = 100$, filter at its maximum weight (d).

Using a filter with small values of k ($\forall k \in \mathbb{R} : k \neq 0 \wedge k \ll 1$) *vwSMAPE* tends to have the same behavior of *SMAPE* about high peaks treatment, but with the huge benefit to avoid *NaN* when both inputs are zero. Fig. 4 shows macro behavior of the *wSMAPE* filter.
The value 1100 in (6) is selected in order to limit the boundary of the filter *Quality Factor* δ. For values of $\delta < 10$ *vwSMAPE* starts to diverge from *SMAPE* behavior up to the maximum weight of the filter, when $\delta = 0$. As showed in both plots of Fig. 5.

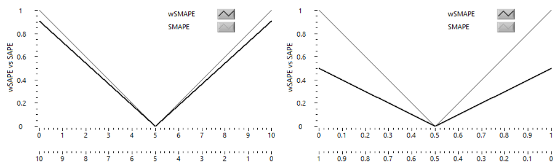

Figure 5. *SAPE* vs *wSAPE* ($\delta = 0$), for input values <10 (left) and <1 (right)

If $10 \leq \delta < +\infty$ thus *wSMAPE* has the same behavior of *SMAPE* for the same aforementioned *x*, *y* input values, as showed in Fig. 6.

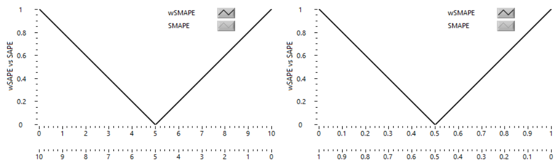

Figure 6. *SAPE* vs *wSAPE* ($\delta = 21$), for input values <10 (left) and <1 (right)

These graphs, Fig. 5 and Fig. 6 show also that if $10 \leq \delta < +\infty$ *wSMAPE* maintains the first kind of symmetry of *SMAPE*, that's inverting *x*, *y* (actual and forecast) the result is the same.

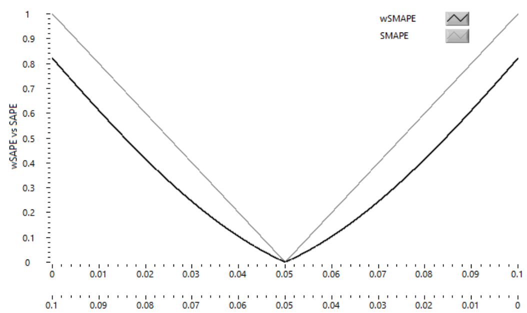

Figure 7. *SAPE* vs *wSAPE* ($\delta = 21$), for input values <0.1

When $k = 50$, for small x, y values (below 0.1), the *filtered wSMAPE* starts its action, Fig. 7, maintaining the symmetry for the x, y inversion.
When the actual value is 100 units, the loss function plot Fig. 8 permits to extend the comparison analysis between *SMAPE* and *wSMAPE* to the second kind of symmetry. As we know from [9] the loss function of *SMAPE* has an asymmetric behavior and when the *wSMAPE* filter reaches the maximum weight, for $\delta = 0$, the difference in Fig. 8 is very small compared to *SMAPE*.

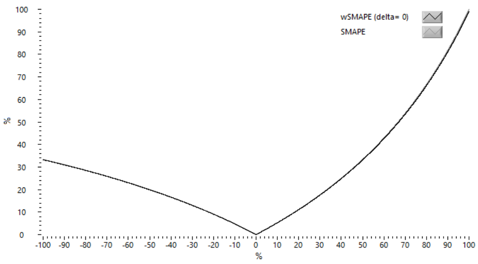

Figure 8. *SAPE* vs *wSAPE* ($\delta = 0$) loss function

To better measure the difference between *SMAPE* and *wSMAPE* loss functions, a plot of these metrics in percentage points for various error levels could help to appreciate discrepancies. A scale magnification is needed to amplify small delta values, for this reason the error percentage points scale in Fig. 9 is plotted in logarithmic.

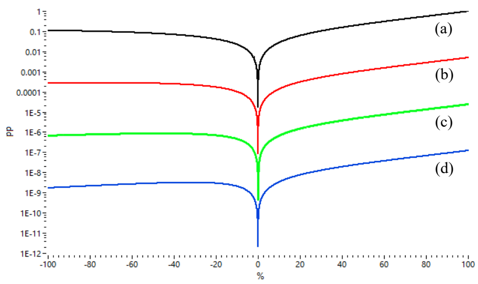

Figure 9. *SMAPE* vs *wSMAPE* delta loss function. *wSMAPE* with $\delta = 0$ (a), $\delta = 1$ (b), $\delta = 2$ (c), $\delta = 3$ (d)

wSMAPE underestimates in both directions, in case of negative percentage errors and in case of positive percentage errors.
When $\delta = 0$, the maximum difference is ≅0.98 pp; when $\delta = 1$ the maximum difference is ≅5E-3 pp; when $\delta = 2$ the maximum difference is ≅2.5E-5 pp; when $\delta = 3$ the maximum difference is ≅1.2E-7 pp, and so on.

Resuming: in the worst case, when $\delta = 0$ and the filter is at its maximum weight, *wSMAPE* underestimates below 1 percentage point the *SMAPE* loss function at the bounds. Increasing δ the more is the reduction of percentage points differences and the more *wSMAPE* approximates *SMAPE*.
For this reason, for a robust and efficient filter behavior, $\delta = 10$ is selected as minimum value. When $\delta \geq 10$ we can consider the invariant property of *wSMAPE* bounds compared to *SMAPE* metric, with the exceptional benefit to control values close to zero, adapting the filter action to the nature of data using *vwSMAPE*, avoiding the problem of undefined values for zero. When the actual value is 0 units is possible to study the difference between *SMAPE* and *wSMAPE* loss functions, Fig. 10, varying the *wSMAPE Quality Factor* δ.

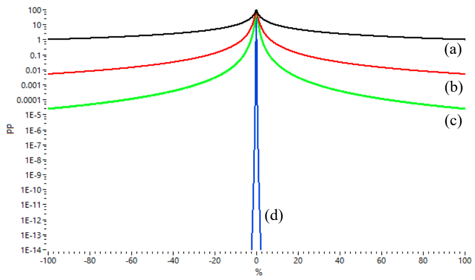

Figure 10. *SMAPE* vs *wSMAPE* delta loss function. *wSMAPE* with $\delta = 0$ (a), $\delta = 1$ (b), $\delta = 2$ (c), $\delta = 21$ (d)

Increasing the value of *Quality Factor* shows how filter grows into a high slope notch, reducing the bandwidth centered in 0. Considering that the value $\delta = 21$ corresponds to *fwSMAPE*.

4 A practical application of *wSMAPE* in loudspeakers *BL(x)*

A Ø50 mm voice coil loudspeaker *BL(x),* with the current offset $x_{off} = 0$, is showed in Fig. 11 and related *BL asymmetry* (A_{BL}) plot is showed in Fig. 1.
Commonly rest position asymmetries generate dynamic DC displacement and Intermodulation Distortion (IMD). Now using the new *wSMAPE* metric, we can measure the value of the *BL* asymmetries related to the position of coil offset, we can call this measure *Mirror* (or *Offset) Asymmetry* [10]; as we know from [4] they generate asymmetrical nonlinearity principally with 2nd-order IMD and Harmonic Distortion (HD).

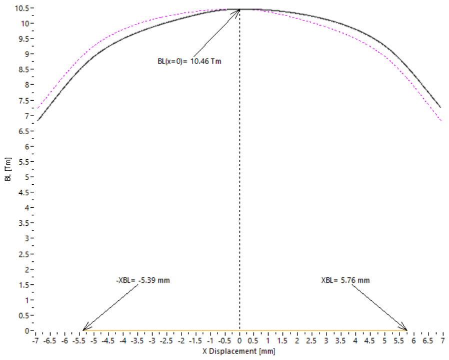

Figure 11. Loudspeaker *BL(x)*

BL Mirror Asymmetry related to Fig. 11 is visible in Fig. 12, obtaining a point-by-point plot (red line) and also a unique value integrated inside the *XBL* region (light grey area). Considering then

$$\lim_{L\to 1} BL(\pm x)\ MirrorAsy. = B(\pm x)\ MirrorAsy. \qquad (7)$$

where L is the voice coil length, (7) permits to study magnetic flux *B* mirror asymmetries using the same equations given in section 3. The ideal loudspeaker has the red line coincident with 0 % line, it means no asymmetries. In this case asymmetries inside *XBL* (@BL_{min}= 82 %) region are 1.04 %.

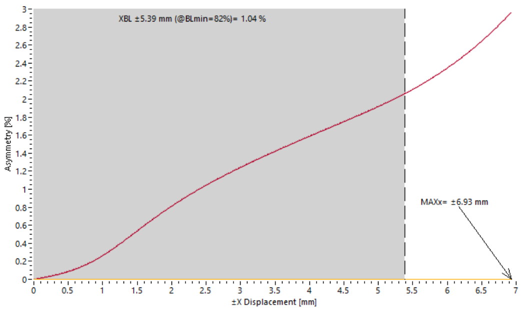

Figure 12. *BL Mirror Asymmetry* @$x_{off} = 0$

Introducing also the new expression *MAXx* (±6.93 mm), it is visible as a yellow line on the base of Fig. 12, it is defined as the *Maximum Available mechanical eXcursion* given at x_{off}.
If the sampled magnetic air gap length is the real max available mechanical space for the voice coil displacement, we can always consider $MAXx \equiv X_{mech}$ (as defined in 15.2.3 of the IEC 62458 [1]). When $x_{off} \neq 0$ a reduction of *MAXx* will occur as visible in Fig. 16 and Fig. 19, respectively ±6.75 mm and ±6.66 mm.

Moreover, formally $XBL \leq MAXx$, particularly *XBL* takes the same value of *MAXx* when a virtual offset is moved near the extreme bounds compared to current rest position, so during displacement peaks.

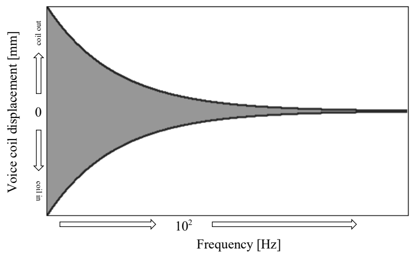

Figure 13. Typical loudspeaker voice coil linear excursion

Keeping in mind loudspeaker rest position is always dominated by highest excursions, statistic distribution of voice coil peaks amplitude depends on applied voltage, music type and loudspeaker application. In addition, the amplitude of displacement is frequency dependent, Fig. 13, so cross-over filters, DSP and limiters impact on peaks.

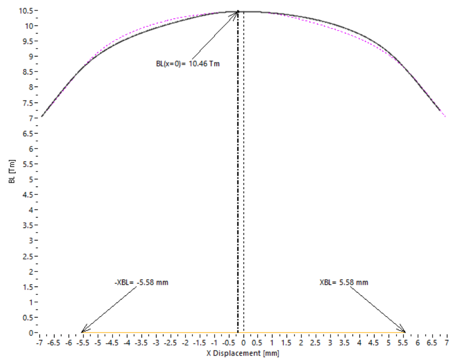

Figure 14. Loudspeaker *BL(x)* @$x_{off} = 0.18\ mm$

Now referring to Fig. 11, a virtual shift of the offset $x_{off} = 0.18\ mm$ permits to obtain the ±*XBL* identity @±5.58 mm as visible in Fig. 14.

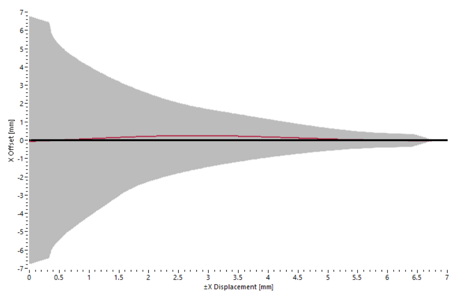

Figure 15. *BL asymmetry* graph @$x_{off} = 0.18\ mm$

Likewise, the identity is observable in Fig. 16 in which at the same *XBL* displacement the mirror asymmetry curve has a null. Pay attention that the perfect symmetrical identity is not set at maximum peak (±6.75 mm), anyway $x_{off} = 0.18\,mm$ reduces mirror asymmetries inside the *XBL* (BL_{min}= 82 %) region from 1.04 % to 0.44 %.

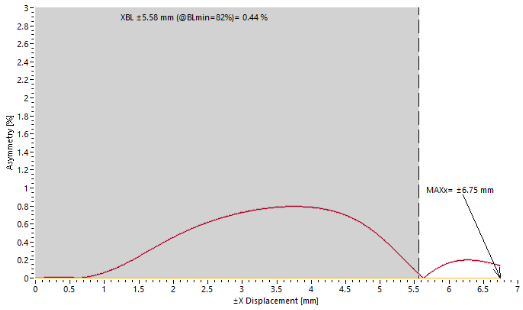

Figure 16. *BL Mirror Asymmetry* @x_{off} = 0.18 mm

The peak of the asymmetry along the red line is given at ±3.8 mm, in which we measure 0.8 %, consequently the asymmetrical *BL* nonlinearity when voice coil displacements cross this point contribute to 2nd-order IMD and HD. Now adding +100 µm to the virtual offset $x_{off} = 0.28\,mm$, Fig. 17 and Fig. 18, we obtain an improved symmetry correlated to BL_{min}= 82 % region measured in Fig. 19.

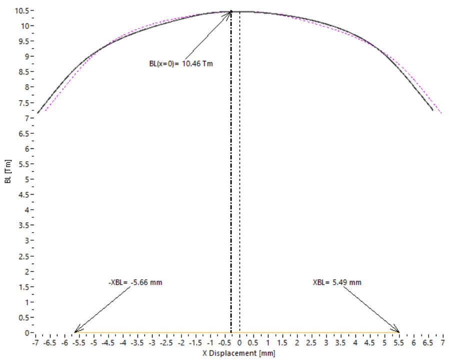

Figure 17. Loudspeaker *BL(x)* @$x_{off} = 0.28\,mm$

From Fig. 19, now *XBL*= ±5.49 mm (@BL_{min}= 82 %) is reduced of -9µm if compared to Fig. 16, then outside the *XBL* (@BL_{min}= 82 %) region the mirror asymmetry curve increases, while inside the *XBL* (@BL_{min}= 82 %) region the asymmetries are near the half of value, they pass from 0.44 % to 0.27 %.
This means that for a certain amount of voice coil displacement, the loudspeaker with 0.28 mm offset has a relative improved nonlinear distortion compared to 0.18 mm offset.

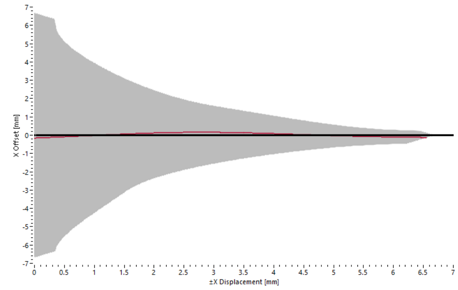

Figure 18. *BL asymmetry* graph @$x_{off} = 0.28\,mm$

Analyzing in deep this specific case in large signal domain, we can see in Fig. 19 a null occurs at x_{displ}= ±4.72 mm and evaluating how the asymmetry curve grows after this point, we can expect that for voice coil displacements below x_{displ}= ±5.2 mm the theoretical improved nonlinear distortion is accurate.

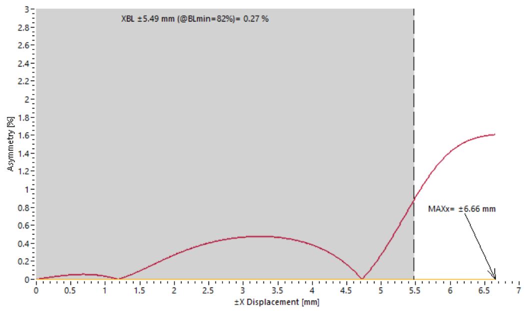

Figure 19. *BL Mirror Asymmetry* @x_{off} = 0.28 mm

When displacement peaks exceed ±5.2 mm, the rising asymmetry curve linked to steeper slopes of force factor curve in Fig. 17 shifts the dynamic offset compared to the selected virtual rest position $x_{off} = 0.28\,mm$, increasing the predicted asymmetry of 0.27 % too.
Note, considering the maximum voltage applied to loudspeaker connectors, the above examination is particularly true for music tracks with a higher degree of dynamic compression, dense of the highest peaks, with a low frequency content, distributed in a time unit; while could be less true for older tracks, not remastered and with a high dynamic content, like some music performances having sparse highest peaks sampled in a time unit.
“Less true” means the rarer are the highest displacement peaks the lesser could be the influence of *BL* asymmetries near the end of the available max displacement, so a better symmetry for certain lower displacements could have more impact on nonlinear distortion averaged in the total time span.

It is noteworthy that all previous selected rest positions x_{sym} points on related A_{BL} graphs (Fig. 1, Fig. 15 and Fig. 18) preserve the absolute value of A_{BL}< 5 %, so they satisfy the A_{BL} "grey region"; but now using the new *BL Mirror Asymmetry* with *wSMAPE* metric it is possible to see in deep mirror differences, measuring them and selecting the setup that best fits for the application.
Moreover, the percentage scale is an absolute quantity, making it useful for comparing different loudspeakers, optimizing or selecting among various designs of the same loudspeaker.
For the mirror asymmetry a limit value is not given, below which to stay to reduce a certain level of distortion, the level is left to the discretion of the designer based on evaluation of all loudspeaker design factors.

5 Conclusions

Introducing a new metric, *wSMAPE*, used here to investigate loudspeaker non-linearities due to *BL(x)* asymmetries. The *wSMAPE* scale-independency permits to compare results among different loudspeakers, optimizing loudspeaker design. The results are point-by-point or averaged, depending the use respectively of *wSAPE* or *wSMAPE* formula, particularly the last one gives a unique number integrating the mirror asymmetries of a specific region. It is possible to use *wSMAPE* metric in loudspeaker field to measure asymmetries (*BL(x)*, *Kms(x)*, etc) or in general to evaluate accuracy of measures. The percentage scale result is an absolute quantity so it represents a powerful instrument for loudspeakers design.
Both *fwSMAPE* and *vwSMAPE* metrics can be used to replace the current well known *SMAPE*, controlling data series having zero and close to zero values. The new *wSMAPE* metric solve also the problem of intermittent data series that produce undefined values, so the practical benefit is to avoid *NaN* when both input values are zero.
Selecting the fixed filter *fwSMAPE* can immediately replace *SMAPE* in all current software or algorithms, while to replace *SMAPE* using *vwSMAPE* into existing systems it is necessary to add the variable k, for controlling the filter weight, adapting it to the process and data typology.
vwSMAPE is a very flexible tool for filter fine tuning, because of k. When replacing *SMAPE* with the new *vwSMAPE*, k permits to switch off the filter ($k = 0$, or at least $k \cong 0$ if a division by 0 is not allowed) making it possible to compare results between *SMAPE* and *vwSMAPE* directly, using all existing input variables avoiding to implement extra software code.
The presented metric offers an instrument helping to enhance loudspeakers motor design and to decide for the optimum x_{sym} point correlated to the limiter of the max displacement peak; especially depending on the loudspeaker type (sub-woofer, woofer, mid woofer, midrange) and its specific application (professional, public address, hi-fi or automotive).

Future study: a *tracking filter* (*twSMAPE*) is under assessment.

References

[1] IEC EN 62458 Standard, *Sound system equipment - Electroacoustic transducers - Measurement of large signal parameters*

[2] Klippel W., *Diagnosis and Remedy of Nonlinearities in Electrodynamical Transducers*, 109th AES Convention, Los Angeles, September 22-25, preprint 5261, (2000)

[3] Klippel W., *Assessment of Voice-Coil Peak Displacement XMAX,* J. Audio Eng. Society vol. 51, Heft 5, p. 307-323, (2003)

[4] Klippel W., Tutorial: *Loudspeaker Nonlinearities - Causes, Parameters, Symptoms*, J. Audio Eng. Society 54, No. 10 pp. 907-939, (2006)

[5] Klippel W., AN 1 *Optimal Voice Coil Rest Position*

[6] Armstrong J. S. *Long-range Forecasting: From Crystal Ball to Computer*, 2nd. Ed. Wiley. ISBN 978-0-471-82260-8, (1985)

[7] IEC EN 60268 Standard, *Sound system equipment - Part 5: Loudspeaker*

[8] Hyndman, R. J., Koehler, A. B., *Another look at measures of forecast accuracy*, International journal of forecasting, 22(4), 679-688, (2006)

[9] Goodwin P., Lawton R., *On the asymmetry of the symmetric MAPE*, International Journal of Forecasting 15, 405-408, (1999)

[10] SpeakerLAB *Virtual Voice Coil* 2.0